Contents

1 Final report

1.1 Project details

Project title	Lidar detection of wakes for wind turbine optimization
Project identification	64016-0020
Name of the programme which has funded the project	Vindkraft
Project managing company/institution	Windar Photonics A/S, Helgeshøj Alle 16-18, 2630 Taastrup
Project partners	DTU Wind Energy
CVR	32157688
Date for submission	

1.2 Short description of project objective and results

The objective of the project “Lidar detection of wakes for wind turbine optimization” was to make nacelle mounted, forward-looking wind lidars with a limited amount of beams deliver robust signals for wind turbine control in wake situations. This objective was met and the lidars by Windar Photonics now includes a robust wake detection algorithm.

Wake situations also create high mechanical loads on the turbine, which in turn can lead to costly repairs and production losses. How to operate the wind turbine in wake situations is therefore also an important question. In Lidar detection of wakes for wind turbine optimization, we have investigated how to alleviate loads while maintaining a high level of electricity production. Our results point to potential gains regarding less loads on the turbine if the wind turbine is yawed relative to the wind direction.

1.3 Executive summary

The ”Lidar detection of wakes for wind turbine optimization project” initiated in October 2016 in collaboration between DTU and Windar Photonics A/S aimed at characterising the wake from an upstream wind turbine with a nacelle mounted Lidar in order to develop a strategy to alleviate loads on the turbine the Lidar is installed on while keeping its power output.

The project was separated into several work packages including the Development of a wake detection algorithm, the test and verification of this algorithm on real world installation, a turbine simulation part and the compensation of the wind direction in wake situations. Finally an administrative work packages was dedicated to project management.

Throughout the project the wake detection algorithm has been successfully developed, tested and documented in journal and conferences papers [1], [2]. The development of this algorithm went through several iterations in order to fit the theoretical initial strategy to real world data gathered on several wind turbines subject to different terrain complexity. Some turbine and compensation strategies have also been investigated and documented in journal and conferences papers [3], [4], [5]. Unfortunately due a change of plan the V52 turbine at Risoe DTU originally planned to test the wake compensation strategy could not be used so that the final testing has been delayed. The potential of the yaw strategy potential had then to be tested in supervised on-site experiments rather than in a full-scale experiment. It will also take place with some commercial partners of Windar Photonics A/S. All the milestones from M1 to M4 could thus be achieved but the milestone M5 has to happen outside the project timeline.

Despite the lack of final testing the project was a success and had lead Windar Photonics to increase its business focus in this area as wake problems are a major issue in the industry that is so far not addressed at a turbine level. It has been proven throughout this project that the wake effects from an upstream turbine can be effectively measured by a Lidar (see 1.5.1) and that following a certain yaw strategy while those effects were occurring lead to a load alleviation on main components of the turbine (see 1.5.8). Provided that the experiment about to happen with Windar’s commercial partner confirms the project’s findings it will result in additional visibility of the Windar products on the market thanks to their unique features. Furthermore, in order to mitigate the effect of not having access to the V52 wind turbine at DTU Risoe, Windar came up with the idea to adapt its current WindTimizer technology to implement a given yaw strategy as explained in 1.6. This means that the current solution can be implemented not only towards the wind turbine manufacturers market but also the retrofit market as no change in the turbine controller is necessary when using the WindTimizer. It thus gives Windar a unique advantage to lead this market.

1.4 Project Objectives

Windar Photonics A/S sells two lidars to the wind turbine industry; the WindEye lidar with two beams and the WindVision lidar with four beams. The lidars are placed on the nacelle of the lidar and the laser beams are focused ahead of the turbine and measure the wind before it hits the turbine. The output of the lidars is primarily used for optimizing the alignment of the wind turbine to the wind direction. However, when the wind turbine is in a wake of a different turbine, the original measurement principle behind the lidar instruments fails and the lidar signals cannot be trusted to the yaw the turbine correctly.

The overall objective of the project was to make the products by Windar Photonics deliver reliable information to the control system of the wind turbine also in wake situations.

This objective was split into three parts:

- Wake detection using WindEye and WindVision lidars.
- Wake compensation; once a wake has been detected, information on the true wind direction should be obtained.
- Wake opitmization investigating how to optimize production and alleviate loads in situations where the wind turbine is in wake.

The project work was originally structured into five work packages, in which the project members worked towards carefully formulated mile stones and deliverables. In parallel, meetings for all project members were organized approximately monthly to bi-monthly throughout the project. The three goals stated above became clearer during the project and towards the end of the project, the reporting and work towards these goals were in the center of all meetings.

Important smaller steps in the project were formulated into five mile stones and six deliverables. Below, each milestone and deliverable is stated. All deliverables and mile stones have been met; however, those marked in yellow were performed in a different way than foreseen when writing the proposal.

M1	First generation wake detection algorithm validated	
M2	Final wake detection algorithm validated	
M3	New experiments finished	
M4	Analyses completed and optimal controller developed	
M5	Final controller algorithm validated	
D1	Release of first generation wake detection algorithm	
D2	Release of final wake detection algorithm	
D3	Documentation of experiments	
D4	Report on wake optimization controller	
D5	Business case demonstration at AWEA/EWEA exhibitions	
D6	Release of wake compensation algorithm	

Table 1: List of milestones and deliverables

One unexpected problem was that the wind turbine controller in the DTU wind turbine for the experiments towards M5 and D4 could not be replaced with the control algorithms developed in the project. At first, we saw this difficulty as a delay, whereas later on it became clear that the validation experiments could not be performed as planned. We explored an alternative validation experiment, using the wind turbines at an American test site in Lubbock, Texas. Although the American partners for this work were keen on the collaboration and tests, these turbines had scheduled repairs and developments during the possible project time window. In the end, we worked with testing of the DTU turbine as originally planned. Rather than implementing the developed algorithms into the controller of the turbine, the developed control settings were tested in supervised on-site experiments. The results from this work, together with extensive computer simulations allowed us to conclude that the developed algorithm has strong potential.

The highest risk was considered in conjunction with the work towards D6 and this anticipation turned out to be true. The original plan was to use so-called Kalman filtering, by which successive readings

of wake affected lidar measurements are used to estimate the exact location the wake. Although this approach is promising, it was too complicated and in October 2018, we had to give it up and focused instead on a simpler method that can easily implemented in the lidar software.

Concerning D4, the wake optimization controller was presented at the WindEurope 2018 Conference at the Global Wind Summit and at the WindEurope Conference and Exhibtion in April 2019, whereas the D5 deliverable was marketed at the largest Wind Energy event in China, “China Wind Power”, in October 2018.

1.5 Project results

This section contains relative detailed information on project methods and results. Dissemination activities (papers and conferences) are summarized in Appendix A.

1.5.1 Wake Detection

Nacelle mounted lidars can be used for remote sensing the inflow of wind turbines. Numerous parameters of the flow can be derived from line-of-sight measurements, namely, wind speed, relative wind direction, effective rotor speed etc. The estimation of these properties assumes a homogeneous wind flow, which is valid in flat homogeneous terrain over large time averages, but is violated in heterogeneous flow condition, such as wake. In wake scenarios, the yaw misalignment measurements from the lidar, deviates significantly from the true value, thus detection and subsequently correction of these measurements is needed. The first step of this project (1) is to identify and quantify the presence of inflow wake using lidar measurements.

The influence of wake in lidar misalignment measurements is illustrated in 1. In an aligned turbine in homogeneous flow (left), the wind speed at the different line-of-sights is equal, thus the measured misalignment is $\phi = 0$. In case of a misaligned turbine (center), the different wind speed at the two line of sights results in $\phi > 0$. In a wake scenario, the wind speed can be different at the two line of sites, even if the flow is aligned, resulting in $\phi > 0$. Figure 1, illustrates a sinusoidal pattern of lidar measured misalignment around the wake sector center.

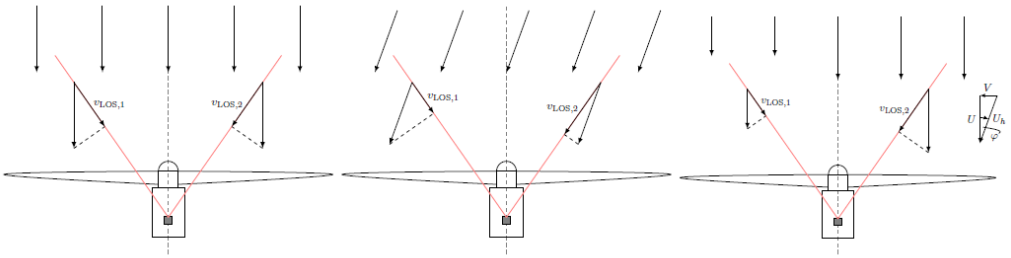

Figure 1: Left: Homogeneous inflow aligned with the turbine. Center: Homogeneous inflow misaligned with the turbine. Right Impinging wake on the left part of the wind field [1]

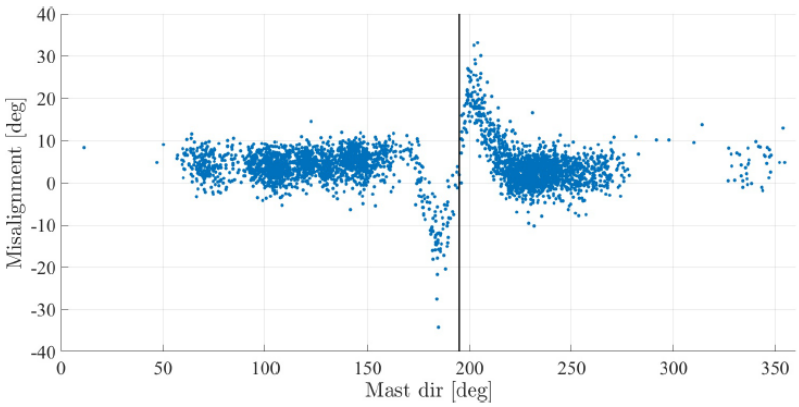

Figure 2: Lidar misalignment as a function of wind direction. Wake sector center at 195^o

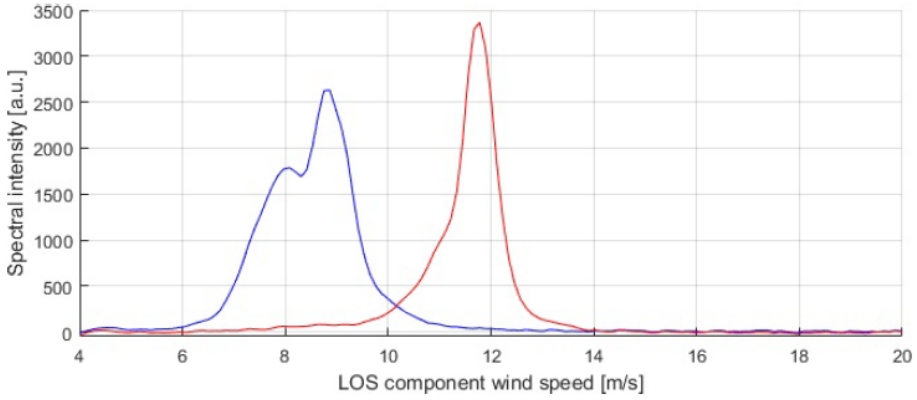

Figure 3: Example of two spectra, where the increased width of the blue spectra is induced by wake

The length-scale of turbulence inside the wake is significant smaller than ambient turbulence [6]. The small scale turbulence contributes to the widening of the Doppler spectrum as experimentally verified by [7]. Figure 3, illustrates a case where one of the laser beams is measuring inside the wake. The small scale turbulence results in increased spectra width. We use the second statistical moment, the spectrum variance, to quantify the wake induced spectra widening. Moreover, the peak of the spectra shifts to the left, indicating lower wind speed compared to the wake free measurement, which can be tracked by the first statistical moment (center of gravity).

Summarizing, the presence of wake, can be detected from a continuous wave laser by tracking the changes in the first and second statistical moment (mean and variance). The line-of-sight turbulence intensity can be derived by normalizing line-of-sight standard deviation (square root of line-of-sight variance) with the line-of-sight speed (wind speed). A wake detection algorithm was developed, that tracks changes in the line-of-sight turbulence intensity and lidar misalignment to detect wake. The algorithm has the ability to detect both partial and full wake situations. In partial wake cases the algorithm can determine which part of the rotor is affected by the wake.

The wake algorithm was developed in the following three sites :

- Risø wind turbine test center. This is a flat, low vegetation terrain where the flow experiences a roughness length change, from water surface to land, in western directions. The experimental setup consists of two turbines: a Vestas V52 with hub height of 44 meters and 50 meters diameter and Nordtank 500 kw turbine with hub height of 36 meters and rotor diameter of 41 m. A WindEYE two beam lidar was mounted on top of Vestas V52 turbine. The distance between the two turbines is 215, which translates into 5.2 rotor diameters at an angle of 195^o. The date come from two different test periods, between 5^{th} December 2015 and 12^{th} January 2016 and between 29^{th} March 2016 and 4^{th} May 2016.
- Tjæreborg wind farm in western Denmark. The site consists of flat, low vegetation terrain. The WindEYE system is mounted on a Vestas V80 turbine. In the vicinity of the test turbine, there are 5 neighboring turbines with diameters ranging from 66 to 80 meters in 3.1 to 7 rotors diameter distance. The test period spans from 5^{th} November 2014 to 10^{th} March 2015.
- A complex terrain site located in Ireland with high elevation differences and dense vegetation. In the vicinity of the test turbine, there are two neighboring turbines, with 80 annd 90 meters rotor diameter, but during the measurements period (11^{th} February to 3^{rd} March), only the wake of the

larger turbine was captured.

Following the algorithm development, the wake detection is verified in a very complex terrain site in Nothern Mexico with Vestas V112. The results presented here, come from the three sites used for development. Figures 4, 5 and 6, illustrate the data the algorithm flagged as wake. It can be seen that the algorithm successfully identifies wake in the infow, for both flat and complex terrain, moreover it can also determine which part of the rotor is affected by the wake. There were very few false detections at the Irish and Tjæreborg site, more specifically 2.3 $\%$ and 1.9 $\%$ for the Irish and Tjæreborg site, respectively. It should be expected that the false detection will be reduced with finer tuning of the algorithm. Figures 7, 25 illustrate the line-of-sight turbulence intensity distribution for Tjæreborg and Irish site and how the measured turbulence intensity increases as the beams scan the wake sectors. It worth mentioning, for the Irish site, that turbulence induced by the forest, southeast of the test turbine, is not detected as wake by the algorithm.

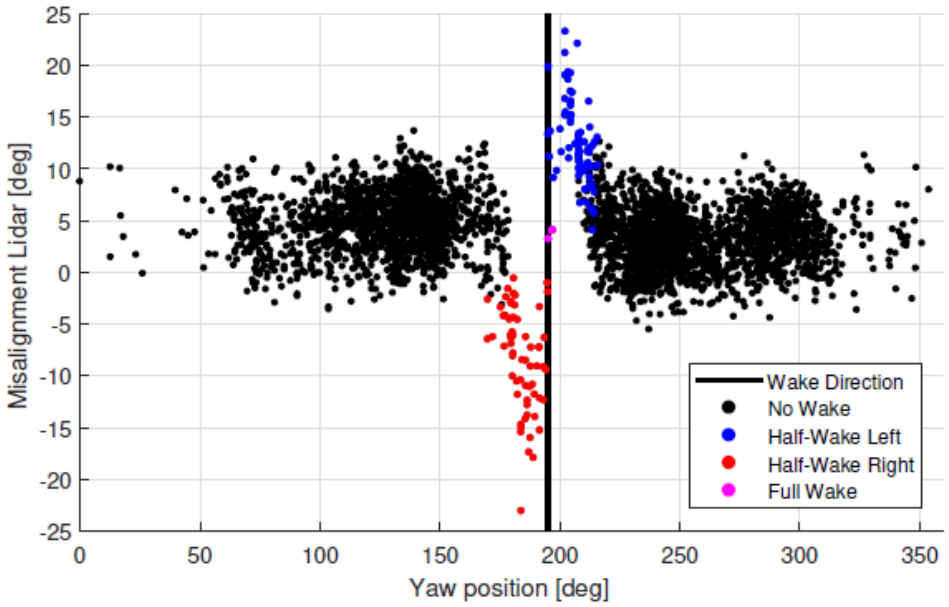

Figure 4: Wake Detection results for Risø test site

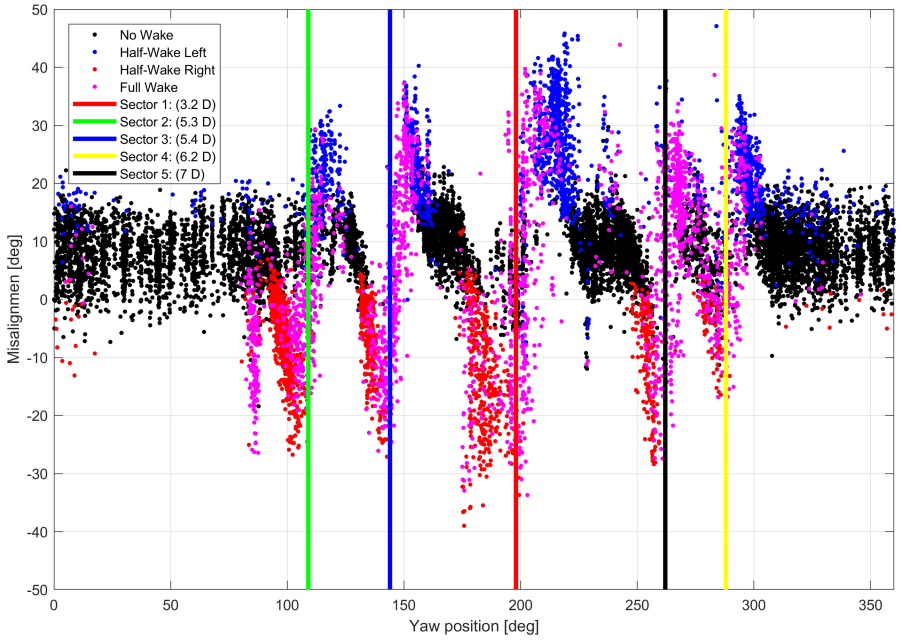

Figure 5: Wake Detection results for Tjæreborg test site

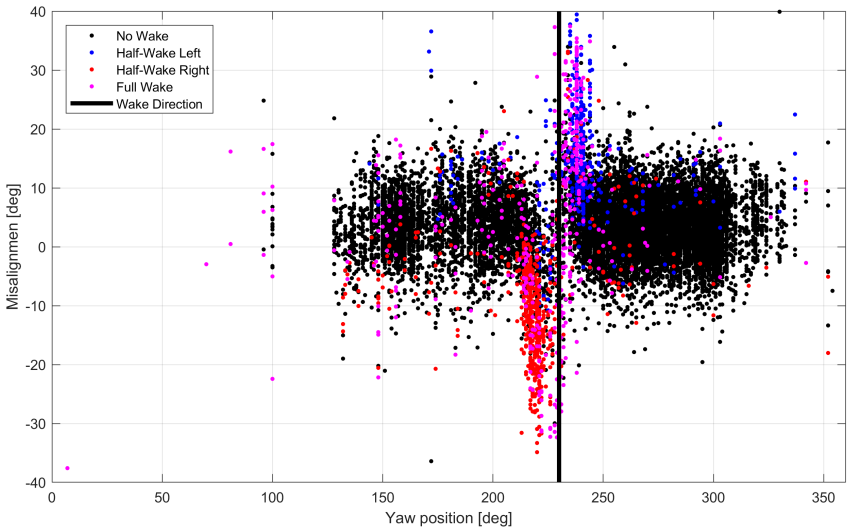

Figure 6: Wake Detection results for Irish test site

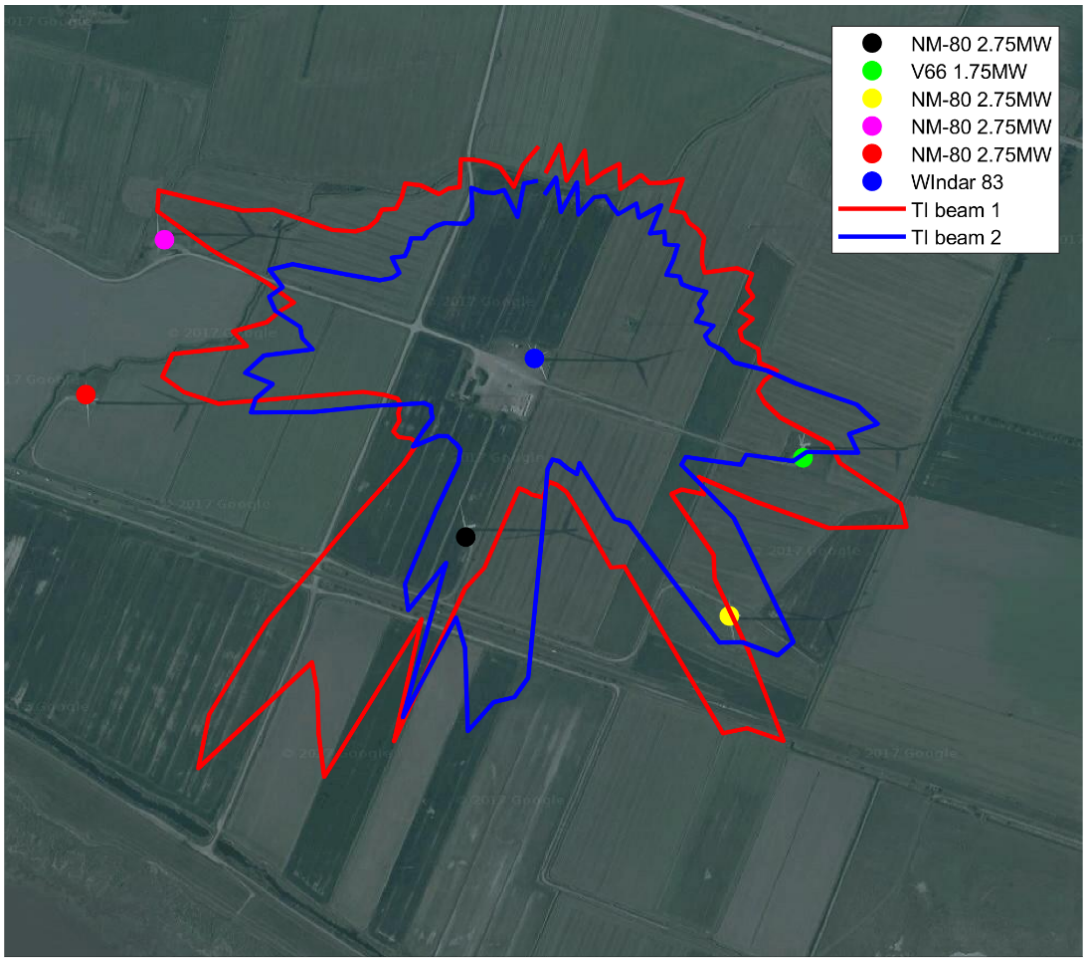

Figure 7: Line-of-sight Turbulence Intensity distribution for Tjæreborg test site

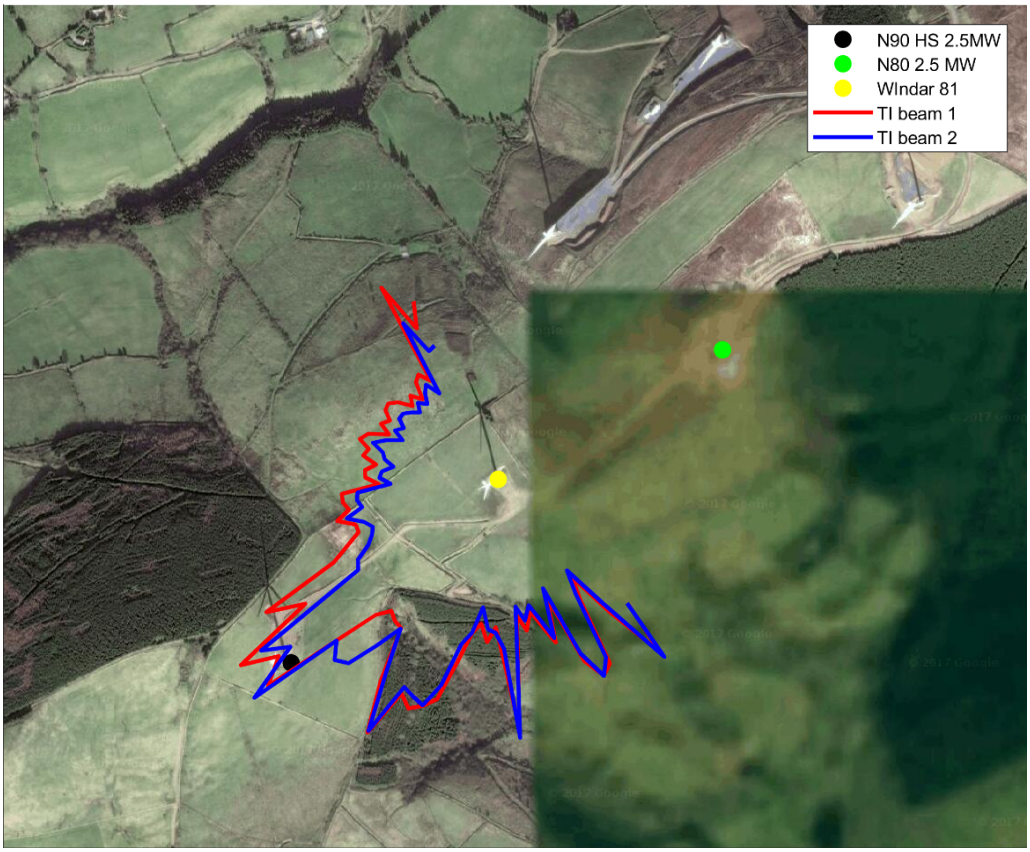

Figure 8: Line-of-sight Turbulence Intensity distribution for Irish test site

1.5.2 Compensation for apparent wind direction change in wake situations

Once a wake has been detected, different solutions for calculating the true wind directions were explored.

1. Switch to nacelle anemometer. By this approach, the wake detection algorithm described above is simply used to determine when the Windar lidar does not provide accurate wind directions.
2. Assume equal wind direction offset as during non-wake situations. By this approach, the knowledge gained from use of the Windar lidar is used to enhance the performance during wake-affected inflow, but similar to approach 1, the strategy depends on the nacelle anemometer.
3. Use empirical data to estimate the true wind direction. By this approach, we assume that we can determine the wind direction by the lidar data alone, using a very simple algorithm. Although the first results were promising, this approach showed to be site dependent and was therefore abandoned.
4. Use of Kalman filtering to deduce true wind direction. By this approach the consecutive readings of wake detection are used to find the true wind direction via an advanced filter. This approach is described in more detail below and in Appendix B.

Introduction to Kalman filtering

The ability possessed by modern wind turbines to actively control the turbine yaw angle offers a means of maintain turbine alignment with the dominant wind direction, thus increasing the power capture [8]. Typically, a yaw control system employs the wind direction measurements from a wind vane that are mounted upon the rear of the nacelle. It is well-known that such yaw misalignment measurements are subject to considerable uncertainties caused by numerous sources such as the rotor-induced flow

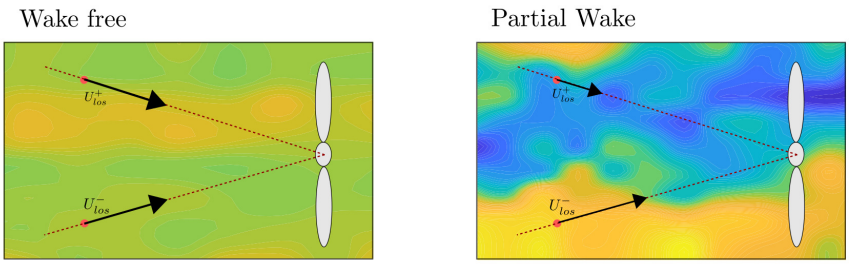

Figure 9: Line-of-sight measurements of LIDAR from a downstream turbine in a wake free and partial wake situation.

distortion [9]. Thus, this has sparked recent interest in improving yaw misalignment using real-time advance measurement technology such as light detection and ranging (LIDAR) systems.

The LIDAR systems provide a sensing of the instantaneous wind speed along a laser beam based upon the Doppler shift effect between the emitted light and back scatter from aerosols in the air. The yaw error could then be computed using measurements from two or more LIDAR beams under the assumption of the homogeneous flow on each height and no vertical and horizontal wind components [10]. These assumptions are reasonable for a terrain that is flat and homogeneous where the ensemble averaged wind speed used to calculate the yaw error depends on the height above the terrain only. In [11], yaw misalignment of the turbine based upon spinner LIDAR measurement was compared against both a nearby reference met mast and a wind vane on the turbine. Later, studies by numerous subsequent authors [12] and [8] also demonstrated that a spinner-based LIDAR could accurately measure the yaw misalignment using simulated and experimental data. Studies by [13] investigated the use of LIDAR measurements on improving the yaw alignment based on simulation modelling. Furthermore, in [14], a full-field test was conducted to show the improvement in the power capture by reducing yaw misalignment based on the LIDAR. In addition, studies by [10] employed the yaw misalignment from a scanning LIDAR to reconstruct the wind veer.

Nonetheless, these studies were based upon a single wind turbine. In a wind farm, the wake is generated by upstream turbines that significantly disturb the downstream wind field properties in comparison to the ambient wind field. Such a wake is typically characterised by a decrease in the mean wind speed (known as the wake deficit) and increase in the turbulence intensity. The wake characteristics violate the assumption of the homogeneous flow as the mean wind speeds in the wake are different to the ambient averaged wind speed. For example, one of the two LIDAR beams is in the wake-free flow regime and the other is in wake affected flow regime. The difference between the two recordings might be misinterpreted as an additional turbine yaw error. To reveal the true yaw misalignment from the LIDAR measurements, it is crucial that the homogeneity of the wind flow remains valid which can be potentially achieved by isolating the wake contributions from the ambient wind field. Therefore, this work proposes a wake tracking algorithm that can estimate the wake location and characteristics and by subtracting the resultant wake deficits from the ambient wind field, the true yaw misalignment can then be recovered. Specifically, such a wake tracking algorithm is developed based on the dynamic wake meandering model (DWM) and extended Kalman filtering approach. The dynamic wake meandering approach characterises the wake as a passive tracer driven by the large-scale turbulence structures in the atmospheric boundary layer [15, 16] and based on the generic wake information, the Kalman filter is employed to estimate the dynamic movement of the wake structure from the LIDAR measurements. The capability of tracking the wake is important from the industrial perspective, since not only the true yaw misalignment can be recovered, leading to an increase in power capture, but also a cost-effective LIDAR is on a par with a spinner LIDAR in a way that the wake characteristics and location can be estimated by exploiting the meandering nature of the wake.

Background and Motivating example

Figure 9 depicts the line-of-sight measurements of the LIDAR from a downstream turbine in a wake and partial wake situation. For brevity, this work only considers a two-dimensional situation, where the wind

flow, wake and LIDAR measurement are at a horizontal plane. The proposed method is self-explanatory to a three dimension situation. In Figure 9, two line-of-sight LIDAR measurements are denoted as U_{los}^{+} and U_{los}^{-}.

A brief introduction of typical yaw error calculation in a wake free situation is presented. Some assumptions are necessary for the problem.

Assumption 1 *The lateral and vertical wind components are negligible comparing to the longitudinal component.*

Based on the Assumption 1, the instantaneous wind speeds in the line of sight (los) of the laser beams $U_{los} \in R$ and the longitudinal wind speed $U \in R$ can be expressed in a relationship via a transformation as follows [10, 17]:

$$U(\mathbf{x}, t) = \bar{U}(\mathbf{x}) + u_t(\mathbf{x}, t) = \frac{U_{los}(\mathbf{x}, t)}{\cos(\theta_p + \theta_y(\mathbf{x}, t)) \cos\theta_t}, \tag{1}$$

where $\bar{U}, u_t \in R$ denote the temporally averaged longitudinal wind speed and longitudinal turbulence component and $\mathbf{x} \in R^3, t \in R$ are a vector representing a point in a three-dimensional space and the time. The LIDAR laser beam pan and tilt angles are denoted by $\theta_p, \theta_t \in R$ whilst $\theta_y \in R$ is the pan-wise turbine yaw error.

The ensemble averaged of (1) is defined as follows:

$$\bar{U}(\mathbf{x}) = \frac{\bar{U}_{los}(\mathbf{x})}{\cos(\theta_p + \theta_y) \cos\theta_t}. \tag{2}$$

Considering the Cartesian co-ordinates $\mathbf{x}$ is converted into polar co-ordinates (r, θ_p, θ_t), where r is the radial distance, it is assumed that two fixed identical LIDAR beams are aiming at the same height (same tilt angle θ_t) with a pair of fixed pan angles $(\theta_p, -\theta_p)$ and their line-of-sight ensemble averaged wind measurements are denoted as $\bar{U}_{los}^{+}(\theta_t) := \bar{U}_{los}^{+}(r, \theta_p, \theta_t)$ and $\bar{U}_{los}^{-}(\theta_t) := \bar{U}_{los}^{+}(r, -\theta_p, \theta_t)$, defined as follows:

$$\bar{U}_{los}^{+}(\theta_t) = \bar{U}^{+}(\theta_t) \cos(\theta_p + \theta_y(\theta_t)) \cos(\theta_t), \tag{3a}$$

$$\bar{U}_{los}^{-}(\theta_t) = \bar{U}^{-}(\theta_t) \cos(-\theta_p + \theta_y(\theta_t)) \cos(\theta_t). \tag{3b}$$

Assumption 2 *The terrain of interest is assumed to be relatively flat, where the wind flow is homogeneous at given altitude and the flow is described by a relatively low Reynolds number.*

Based on Assumption 2, on a flat and homogeneous terrain, the ensemble averaged mean wind speed is only dependent on the height, thus, $\bar{U}^{+}(\theta_t) = \bar{U}^{-}(\theta_t) = \bar{U}(\theta_t)$. By rearranging (3), the turbine yaw error angle can be determined by the following expression [10]:

$$\theta_y(\theta_t) = \arctan\left(\frac{\bar{U}_{los}^{-}(\theta_t) - \bar{U}_{los}^{+}(\theta_t)}{\bar{U}_{los}^{-}(\theta_t) + \bar{U}_{los}^{+}(\theta_t)} \cot\theta_p\right) \tag{4}$$

Motivating example

A downstream turbine experiencing a partial wake situation is demonstrated in the right of Figure 9. It is clearly shown that one of the LIDAR measurements is in the ambient wind flow (illustrated by the colour yellow) whilst the other is in the wake (illustrated by the colour blue), resulting in deficits in wind speed. Such a deficit in the line-of-sight wind measurement could contribute additional error to the turbine yaw misalignment based on (4). In this partial wake situation, the line-of-sight ensemble averaged wind measurements (3) are modified where the ensemble averaged wind speed at the measurement point becomes $\bar{U}^{+}(\theta_t) = \bar{U}(\theta_t) + \bar{U}_w^{+}(\theta_t), \bar{U}^{-}(\theta_t) = \bar{U}(\theta_t) + \bar{U}_w^{-}(\theta_t)$, defined as follows:

$$\bar{U}_{los,wake}^{+}(\theta_t) = (\bar{U}(\theta_t) + \bar{U}_w^{+}(\theta_t)) \cos(\theta_p + \theta_y(\theta_t)) \cos(\theta_t), \tag{5a}$$

$$\bar{U}_{los,wake}^{-}(\theta_t) = (\bar{U}(\theta_t) + \bar{U}_w^{-}(\theta_t)) \cos(-\theta_p + \theta_y(\theta_t)) \cos(\theta_t), \tag{5b}$$

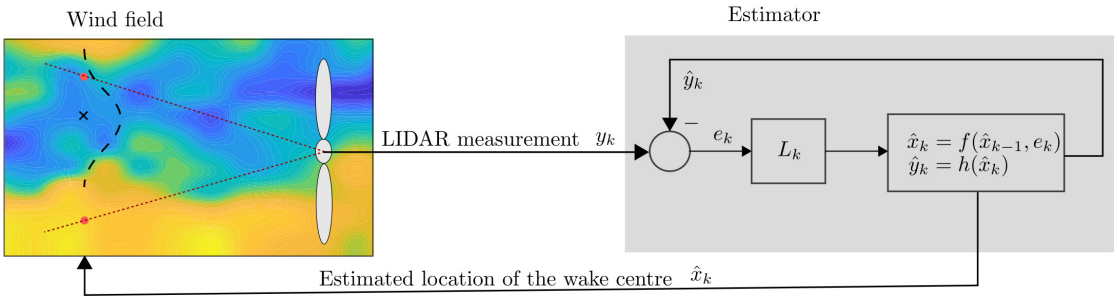

Figure 10: Problem schematic.

where $\bar{U}_w^+, \bar{U}_w^- \in R$ denote the mean wake deficits at the measurement point. This work aims to *track the wake centre location* and then the mean wake deficits at the measurement points $\bar{U}_w^+(\theta_t), \bar{U}_w^-(\theta_t)$ are estimated. Once the mean wake deficits are known and by subtracting them in (5), the line-of-sight wind measurements without the wake influence are defined as follows:

$$\bar{U}^+_{los,nowake}(\theta_t) = \bar{U}(\theta_t)\cos(\theta_p + \theta_y(\theta_t))\cos(\theta_t), \tag{6a}$$

$$\bar{U}^-_{los,nowake}(\theta_t) = \bar{U}(\theta_t)\cos(-\theta_p + \theta_y(\theta_t))\cos(\theta_t), \tag{6b}$$

Thus, with $\bar{U}^+_{los,nowake}, \bar{U}^-_{los,nowake}$, the correct yaw error angle/misalignment can be recovered by (4).

Problem description and methodology

The design of the estimator is depicted in Figure 10. In the left of the figure, it is a snapshot of a turbine located in the downstream and subjected to a partial wake generated from upstream turbines. The wake (decrease in the wind speed) is denoted by the blue colour whereas the ambient wind speed with turbulence is denoted by the yellow colour. The LIDAR provides two measurements of the wind speed, represented by the red dots. One of the measurements is clearly in the wake and another is in ambient wind flow. This could contribute to an additional yaw error as one of the LIDAR measurements is corrupted by the wake. The cross and dash line denotes the estimated location of the wake centre from the estimator and the mean wake deficit Gaussian profile.

In the right of the figure, it is the proposed estimator in the work. Let x_k denotes the true state (location of the wake centre and other wake information) whilst $\hat{x}_k$ represent their estimates. The key role of the estimator is to ensure the state estimate is as close as possible to the true state. The estimator predicts the current estimated wake centre $\hat{x}_k$ by employing the dynamic wake meandering model f and the previous state estimate $\hat{x}_{k-1}$. Based upon the current estimated wake centre $\hat{x}_k$, the estimated wind speed at the LIDAR measurement point $\hat{y}_k$ is computed by using the wake characteristics and sensor dynamics h. The estimated wind speed $\hat{y}_k$ is then subtracted from the actual measurement y_k to form an error signal e_k. This error is then multiplied with the filter gain L_k to introduce a correction term that is used in the dynamic wake meandering model in an attempt to minimise the error signals in the subsequent iterations. Notice that the Kalman filter is a recursive filter and the filter gain is computed that minimises the mean square error $E(x_k - \hat{x}_k)(x_k - \hat{x}_k)^T$ for given measurements y_k, where E denotes the expectation of sequence and $(\cdot)^T$ is the transpose of a vector.

Dynamic wake meandering model and mean wake deficit profile

This section presents the wake models that used in the estimator. The dynamic wake meandering model is based upon a fundamental conjecture that the transport of wakes in the atmospheric boundary layer can be modeled as a passive tracer driven by the large-scale turbulence structures. The meandering process is then described by a stochastic transport media as well as of a suitable definition of the cut-off frequency of the large-scale turbulence structures.

The wake deficit dynamics in the lateral direction can be modelled as follows:

$$\dot{y}^g = v^c, \tag{7a}$$

where the $y^g \in R$ denotes the lateral location of the wake centre, $\dot{(\cdot)} := \frac{d(\cdot)}{dt}$ is the time-derivative and $v^c \in R$ represented the transversal wake transport velocity. This transversal wake transport velocity v^c

is governed by a stochastic/coloured noise and its dynamics is similar to a low-pass filter, defined as follows:

$$\dot{v}^c = -\omega_c v^c + \omega_c n, \tag{7b}$$

where $n \in R$ denotes the white noise and the cut-off frequency $f_c = \frac{\omega_c}{2\pi} \in R$ is determined by the ambient mean wind speed $\bar{U} \in R$ in the longitudinal direction and wake deficit diameter $D_w \in R$:

$$f_c = \frac{\bar{U}}{2D_w} \tag{7c}$$

Next, the mean wake deficit profile is presented where such a model helps the estimator to identify the wake centre based on the wind speed measurement. From empirical studies [15], the downstream mean wake deficit profiles corresponding to an ambient mean wind speed can be characterised as a Gaussian function $g(y^g, \mu, \sigma) : R \times R \times R \to R$ in a far wake situation. The mean wake deficit can be expressed mathematically as follows:

$$\bar{U}_w(y^g, \mu, \sigma, \bar{U}_{peak}) = \bar{U}_{peak} \frac{1}{\sigma\sqrt{2\pi}} e^{-\frac{1}{2}(\frac{y^g-\mu}{\sigma})^2} \tag{8}$$

where $\bar{U}_w, \bar{U}_{peak} \in R$ denotes the wake deficit and its peak relative to the mean ambient wind speed $\bar{U}$ and $\mu, \sigma \in R$ are the mean of the wake deficit and standard deviation of the Gaussian profile.

Assumption 3 *The mean ambient wind speed $\bar{U}$ at given attitude is known, either by estimation or detected by one LIDAR beam in wake free situation. The parameters for the mean wake deficit profiles $\bar{U}_{peak}, \mu, \sigma, D_w$ are assumed to be estimated real-time based on system identification technique or known in advance.*

Design of estimator The estimator design is based on a celebrated Kalman filtering approach [18]. Kalman filter provides the optimal state estimates of a linear systems by minimising the mean square state error or state error covariance matrix $P_k := E[(x_k - \hat{x}_k)(x_k - \hat{x}_k)^T]$. Given the fact that the models discussed in Section 1.5.2 is nonlinear, an extended Kalman filter (EKF) is employed to estimate the states of the system, namely the wake information and centre location. The EKF is similar to Kalman filter except that it computes the estimates based on the nonlinear equations and determines the state co-variance matrix P by linearising around the current state estimate. Notice that the model in Section 1.5.2 is in continuous-time and it is more convenient if the model can be expressed in discrete-time thus a discrete-time EKF can be employed. The notation $f, g : R \to R$ are the discrete-time representations of the dynamic wake deficit meandering model (7) and mean wake deficit Gaussian model (8). The state x_k of the system at sample time k consists of the lateral location of the wake centre, transversal wake transport velocity, defined as follows:

$$x_k := [y_k^g, v_k^c]^T, \tag{9}$$

and the measurement to the estimator consists the wake deficits, that is calculated based on (5) with two LIDAR measurements, defined as follows:

$$y_k := [\bar{U}_w^+, \bar{U}_w^-]^T. \tag{10}$$

Typically, an EKF consists of two steps, prediction and measurement update. Notice that superscripts $x_k^+ := x_{k|k}, x_k^- := x_{k|k-1}$ are used to determine the variable x at sample time k given observations up to and including sample time k for x_k^+ or $k-1$ for x_k^-. The notation x_k^+, x_k^- are also known as the *a posteriori* and *a priori* state estimate.

In the prediction step, the EKF predicts the estimate and error co-variance based on the system models and information from the previous step. The predicted/a priori estimates for the state $\hat{x}_k^-$ and error co-variance matrix P_k^- can be calculated as follows:

$$\hat{x}_k^- = f(\hat{x}_{k-1}^+), \tag{11a}$$

$$P_k^- = F_k P_{k-1}^+ F_k^T + Q_k, \tag{11b}$$

$$F_k := \frac{\partial f(x_{k-1}^+)}{\partial x}. \tag{11c}$$

where the $\hat{x}_{k-1}^{+}$ and P_{k-1}^{+} are the updated/a posteriori state estimate and co-variance estimate from the previous step, whilst Q_k is the noise co-variance matrices to the dynamic model, chosen by the designer.

Next, in the measurement update step, the prediction is corrected by exploiting the measurement, yielding the updated estimates $\hat{x}_k^+$ and error co-variance P_k^+, defined as follows:

$$\hat{y}_k = h(\hat{x}_k^-) \tag{12a}$$

$$\hat{x}_k^+ = \hat{x}_k^- + L_k(y_k - \hat{y}_k), \tag{12b}$$

$$P_k^+ = (I - L_k H_k)P_k^-, \tag{12c}$$

$$H_k := \frac{\partial h(x_k^-)}{\partial x} \tag{12d}$$

where L_k is the filter gain. The filter gain is computed as follows:

$$L_k = P_k^- H_k^T (H_k P_k^- H_k^T + R_k)^{-1}. \tag{13}$$

where R_k is the noise co-variance matrices to the measurements that it is also a parameter tuned by the designers. Subsequently, the estimate of system states (wake information and centre location) $\hat{x}_k^+$ and the mean wake deficits $\hat{y}_k := [\bar{U}_w^+, \bar{U}_w^-]^T$ are the best estimates for measurements up to and including sample time k. At the next sample time, the estimator repeats the prediction and measurement update steps.

In addition, some parameters such as the mean ambient wind speed $\bar{U}$, mean peak wake deficit $\bar{U}_{peak}$, μ, σ and D_w does not hold any dynamics, thus, estimation of those parameters is achieved by some system identification techniques or parameter identification methods such as immersion and invariance-based nonlinear estimator design [19]. The summary of the estimator design is shown in Figure 11.

Conclusions and future work

Given the limited time and resources, this task has not been fulfilled. In the future, the plan is as follows:

1. Numerical simulation in HAWC2 or PyWake with no ambient turbulence and only wake meandering turbulence, assuming some parameters about the mean wake deficit profile such as $\bar{U}_{peak}, \mu, \sigma, D_w$ and the mean ambient wind speed are known.
2. Similar numerical studies with ambient turbulence.
3. Numerical studies with ambient and wake meandering turbulence. The parameters about the mean wake deficit profile are estimated by system identification method.
4. Studies using Full filed measurement. A scanning LIDAR can provide a downstream wake situation in a horizontal plane, similar to the right of Figure 9. The studies could choose two points to represent the cost-effective fixed beam LIDAR. Based on these two points, we can verify if the estimator can estimate the wake centre location correctly.

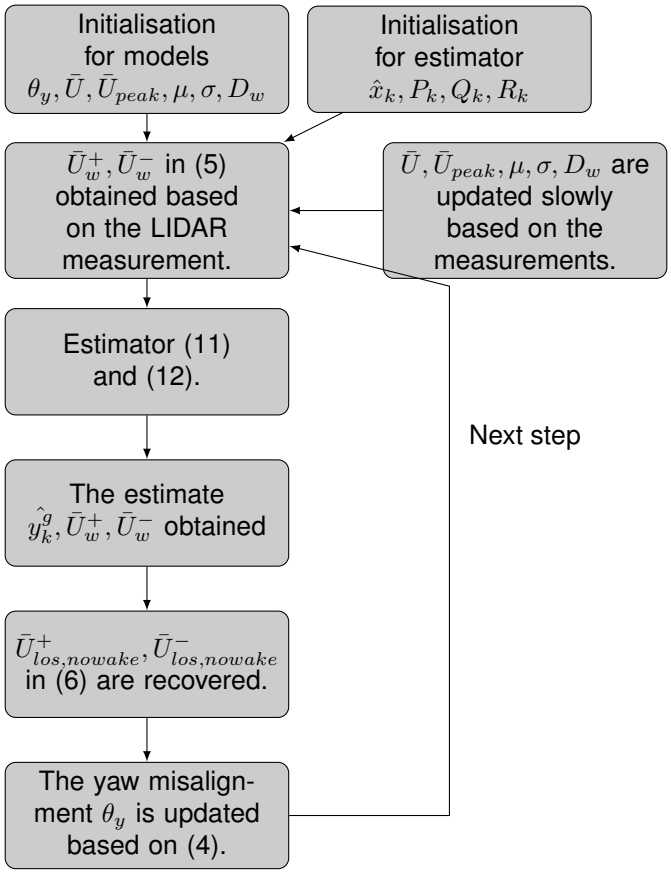

Figure 11: Flow of the estimation algorithm

Turbine optimization in wake-affected inflow

Motivation In a wind farm, the interaction of nearby wind turbines affects the flow, thus the performance of the downstream turbines. Power and loads are influenced by this phenomena where, generally, higher fatigue loads are observed when wake is present. An example can be observed in figure 12 where the blade flapwise and tower top fore-aft moment damage equivalent load (DEL) are plot as function of wind direction.

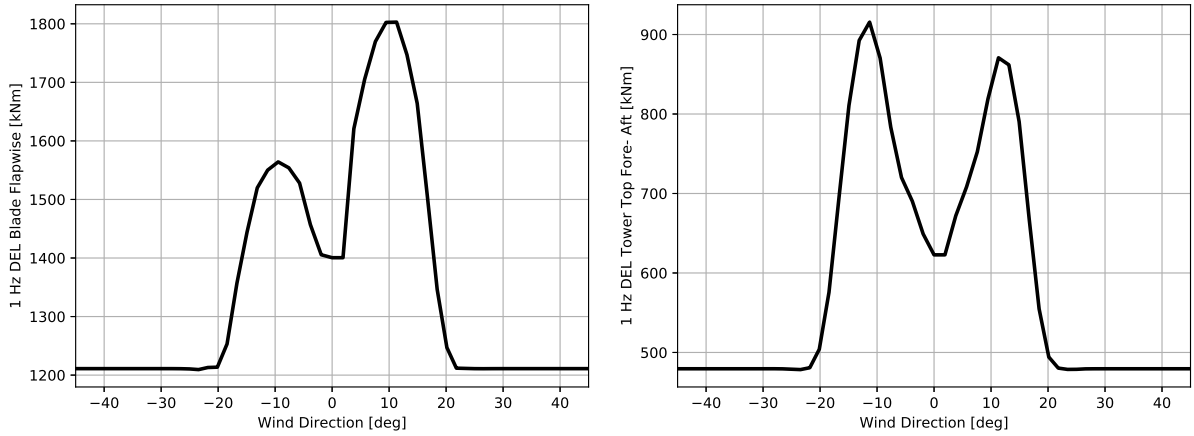

Figure 12: Blade Flapwise Moment and Tower Top Fore Aft DEL for upstream wake at 3D position as function of wind direction for 12 m/s simulation and 5% turbulence intensity

The simulations presented in figure 12 corresponds to a two turbine simulation with a spacing of 3D in the main wind direction and aligned in the transverse direction. Thus, the cases where wind direction is 0, corresponds to full wake cases while for wind turbine misalignment's, i.e. -40 degrees, the upstream wake will not affect the downstream turbine. It is possible then to refer to those cases as a free stream case or non-waked case.

It is possible to observe an increase of the loading when wake is present for both cases in figure 12. For the blade flapwise DEL, left panel on figure 12 an increase of 50% can be observed if a partial wake case (wind direction 10 degrees) is compared to the free stream case. Higher increase, around 80%, are observed in the tower top fore-aft DEL, right panel on figure 12, for the partial wake cases (wind direction $\pm$ 10 degrees) compared to the free stream case.

The main results are summarize in the following sections. 1.5.3 presents the HAWC2 vs experiments comparison where the fatigue load alleviation predicted by HAWC2 is compared with measured data. Then 1.5.6 presents the simulation set-up for the wake scenarios, the yawing and de-rating strategies for load alleviation. Finally, 1.5.7 presents fatigue load alleviation for both presented strategies without compromising power. On the other hand, in 1.5.7 power is compromised to further decrease the wake impact on the loads.

1.5.3 Validation Yaw Strategy for Load alleviation

Load reduction by yawing a wind turbine has been previously been demonstrated by [20] where the potential load reduction on a isolated machine is presented. The work has been extended in this project where the influence of the wake and yaw misalignment for load reduction was studied [3]. The work presented in [3] only present cases where the yaw strategies are defined constrained to maximum power production.

1.5.4 Experiments set-up

The experiments were carried in the V52 at Risø campus between August and December 2018 where the wind turbine was intentionally misaligned while recording loads on the main wind turbine components. The experiment was conducted by provoking an offset on the yaw angle following a sequence of positive to negative angle passing throw 0. In each of the yaw misalignment positions, the wind turbine was operation for thirty minutes.

The idea of this sequence is to enable a comparison of the relative increase/decrease of fatigue assuming similar inflow conditions during one complete yawing sequence (around 150 minutes considering the transients from one misalignment to another). However, when post-processing the results, it was found that the relative change on fatigue loading was smeared out with the variation of atmospheric conditions during the complete yawing sequence.

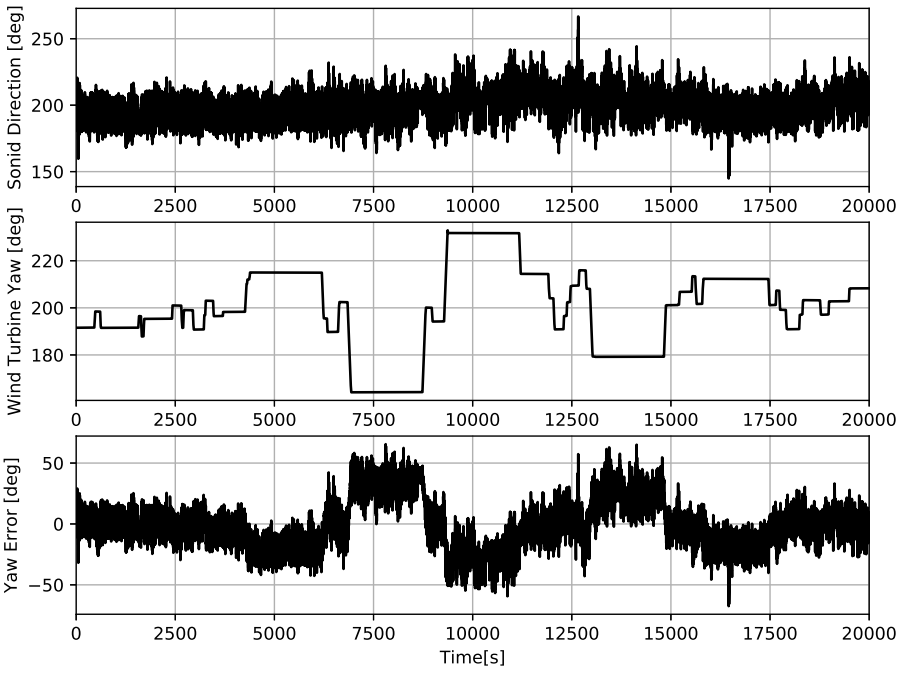

Figure 13: Example on V52 imposed yawing sequence during 16 of August 2018

1.5.5 Validation

The Damage Equivalent Load (DEL) for the experiments was obtained in order to quantify the relative fatigue difference with the aligned case. The data was binned and classified as aligned when the yaw misalignment was comprehended between $\pm$ 5 degrees, obtaining this reference value based on historical data of the turbine during normal operation, and positive or negative misalignment when the binned misalignment is outside the normal operation bound. The reference coordinate system is the same as presented in figure 17. Figure 15 presents the DEL for the aligned and misaligned yaw cases.

The misaligned experiments, following a yawing sequence, was performed to ensure similar inflow conditions which objective was to reduce the inflow variability during the experiments. However, as it can be seen in figure 15, no clear conclusion was found using this approach. From simulations, it is known that in the below rated region, wind speeds lower than 12 m/s, positive yaw misalignment lead to an

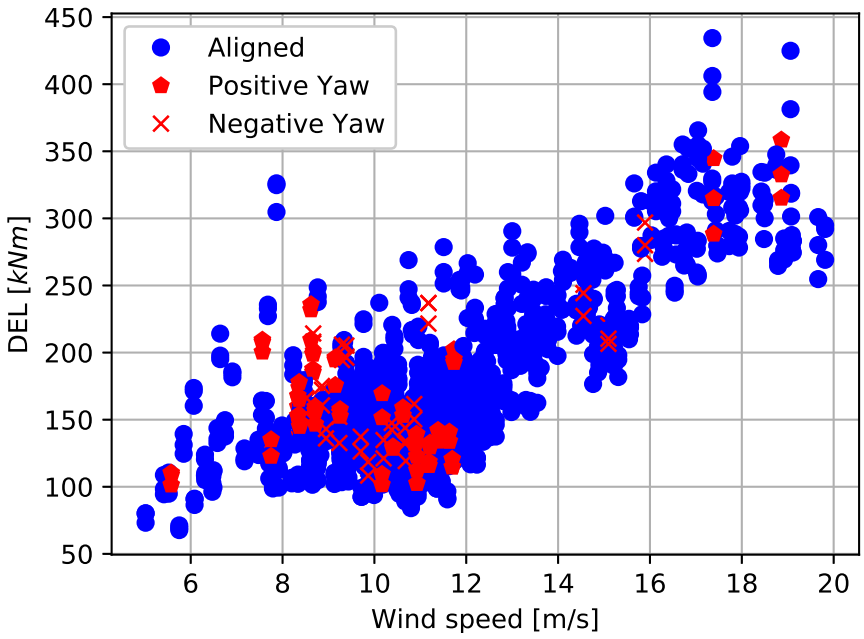

Figure 14: DEL Classification V52 yaw experiments on aligned, positive and negative misalignment

increase of fatigue loading while negative to a decrease. It was not possible to observe this trend in figure 15.

The lack of a large data-set presenting large yaw misalignment combined with the uncertainty of the atmospheric conditions, the load alleviation comparison is always done assuming the same flow conditions, lead to post-process the data in a different manner. Two different approaches were tested on simulated data before its application to measurements. The first approach uses a high-pass filter to remove fluctuations on the wind speed signal. The second approach uses a band-pass filter around the 1P frequency. The 1P frequency corresponds to the rotor speed value of each analyzed time-series. Both methods decrease the uncertainty if compared with the DEL method. An example is shown in figure 15.

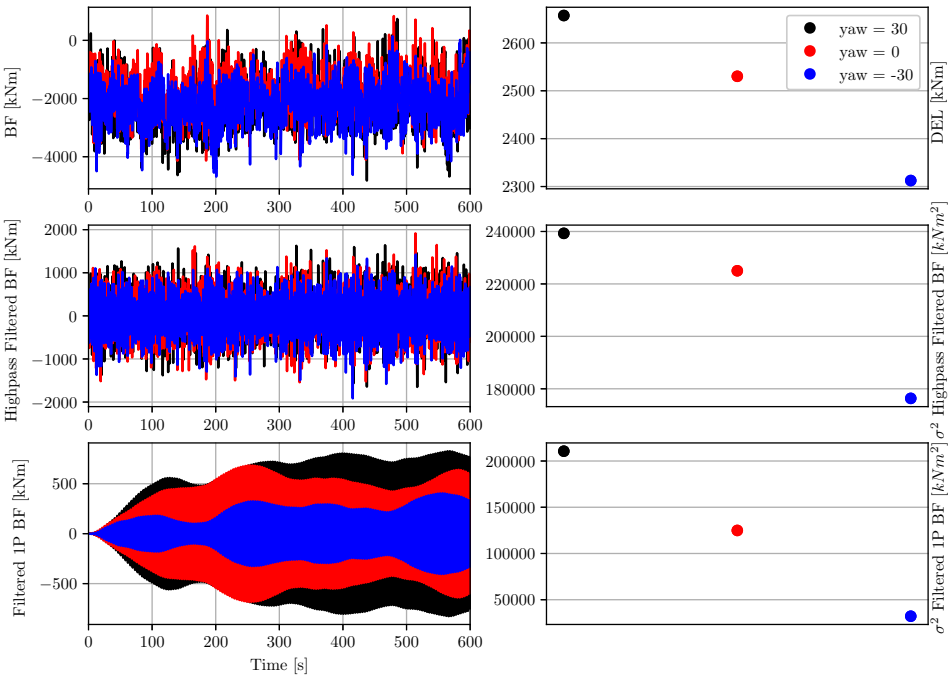

Figure 15: Simulation Example on Blade Flapwise Moment Filtering using High-pass and Band-pass at 1P reference

Figure 15 presents the simulation time-series of the blade flapwise load for an aligned case (red) and misalignment of $\pm$ 30 degrees (black and blue) on the top left panel. The corresponding DEL, where a decrease in value is observed for the negative misaligned case, is shown in the top right panel. Correspondingly, the time-series results of the two proposed methods are shown in the figure with its corresponding alleviation analysis. In this case, signal's variance is used to determine the load alleviation.

It is possible to observe that the trends between the original post-process signal into DEL (top right panel) are the same than the two proposed approaches (middle and bottom right panel). It was decided to post-process the data using the third approach, 1P band-pass filter, since the periodic loading on the 1P is where the yaw misalignment has a higher influence. Based on the measured yaw misalignment, wind speed, shear and turbulence intensity for the free stream sector at Risø campus, HAWC2 simulations has been performed to compare with measurements. Figure 16 presents the variance of the 1P filtered data for simulations (top) and measurements (bottom).

Figure 16 shows a good correlation between simulations and measurements post-processed data where the trends and misalignment outliers match. The increased loading can be easily identified, for example around 11 m/s where negative misalignment or for 18-20 m/s where positive misalignment produced higher loading. The load alleviation is a bit more difficult to observe but some cases around 10-12 m/s and 14-16 indicates the potential of the strategy.

1.5.6 Simulation Set-up

The simulated wind turbine is a collective pitch regulated, variable speed turbine with a rotor diameter of 90 m and a rated power of 2.3 MW at 12 m/s. The wind turbine type and size matches the average

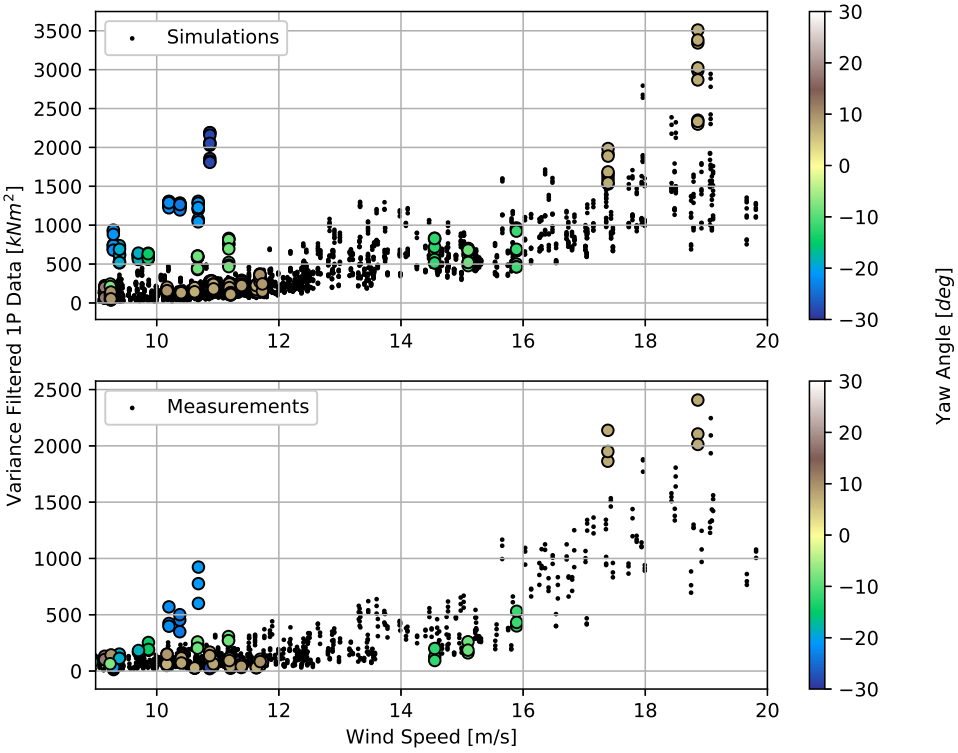

Figure 16: Comparison simulation and measurements variance of Filtered 1P Data on the V52 yaw experiments

machine that Windar Photonics is targeting for the load alleviation add-ons. HAWC2, the inhouse aero-servo-elastic code of DTU Wind Energy, has been used to generate the wind fields and obtain power and loading of the main wind turbine components. Two turbines are used in the setup: the first turbine is used to generate the wake, while the power production and loads are computed on the second turbine. The unsteady inflow conditions are defined on the upstream turbine. Thus, the downstream turbine feels a disturbance of the original inflow due to the wake. It is important to remark that the wake downstream advection direction is not changed, thus, wake steering is not part of this analysis.

The wind turbine spacing as well as the yaw angle of the downstream wind turbine are varied to characterize the effect of yawing in a wake situation. Six ten-minutes simulations with different stochastic realizations (ie. based on different random seeds) per case are used to improve the statistical significance of the results. The investigated scenarios include mean wind speeds ranging from 4 m/s to 25 m/s.

1.5.7 Derated Control Strategy

Proportional derated control is performed at below-rated wind speeds. Proportional derated control refers to changing the power output of the turbine to a proportion of the available power. Two implementations of proportional derating are used to investigate load alleviation as shown in Figure 18. The first method is to alter the minimum blade pitch angle while maintaining the same tip speed ratio. The second method is to alter both the minimum pitch angle and the tip speed ratio using torque control. Both strategies are implemented in at 90% and 80% derating HAWC2 by means of look-up tables.

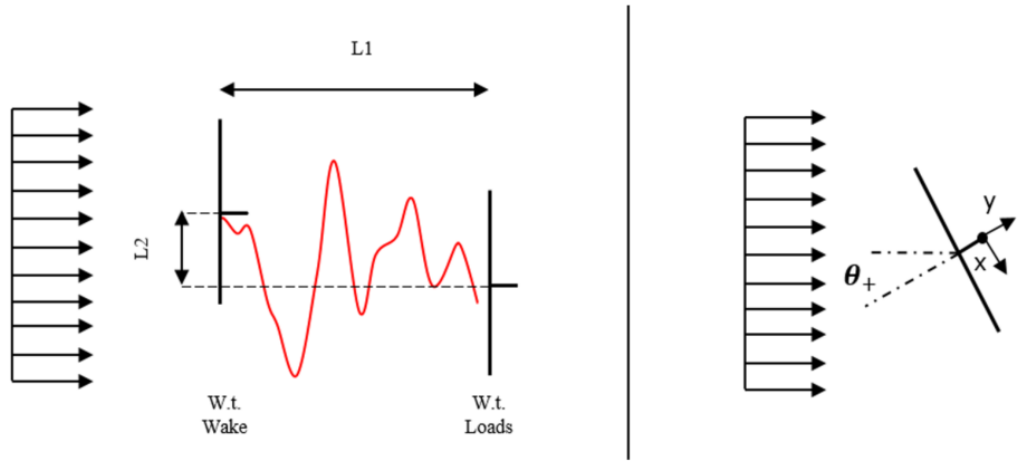

Figure 17: Setup description: left: two turbines configuration; right: turbine yaw convention.

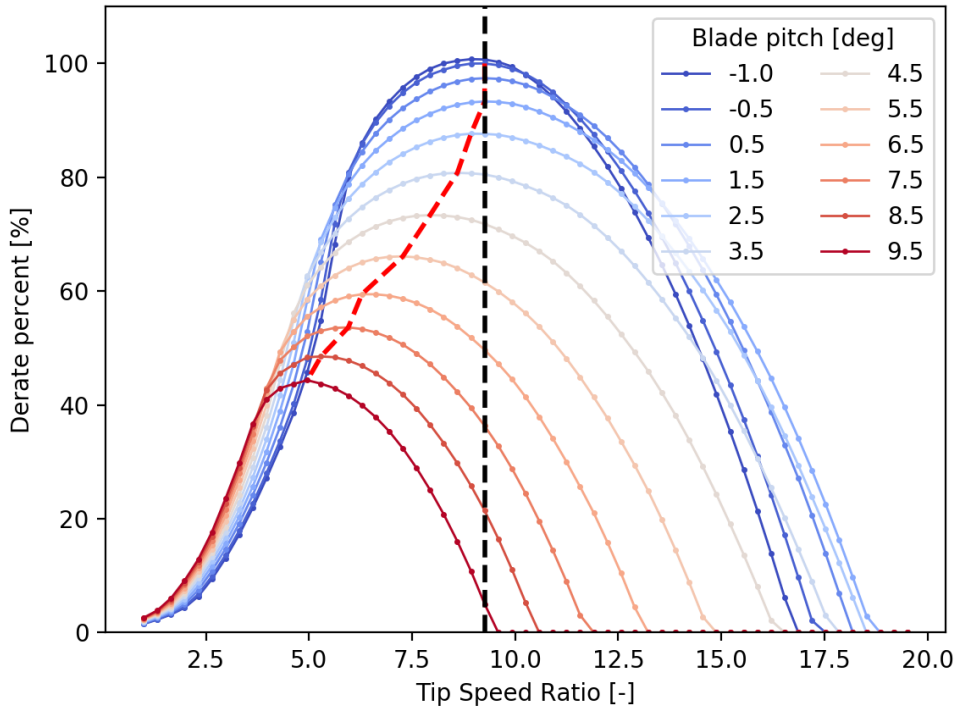

Figure 18: Derating percentage versus tip speed ratio for varying pitch angles. The two implementations of proportional derating are pitch offset (Black dashed line) and pitch offset with torque control (red dashed line).

Optimization with constrained power production

This strategy is only relevant for above rated conditions since yaw misalignment in the below rated conditions will lead to a reduction in power production. The results are dependent on the inflow observed by the downstream turbine which depend on the atmospheric turbulence intensity and downstream position relatively to the closest wind turbine.

The yaw strategies presented in figure 19 are found to minimize the blade flapwise fatigue loading. In principle, any other loading could be used to define the yaw strategy but, during the project, it was found that the loading with higher potential was the blade flapwise.

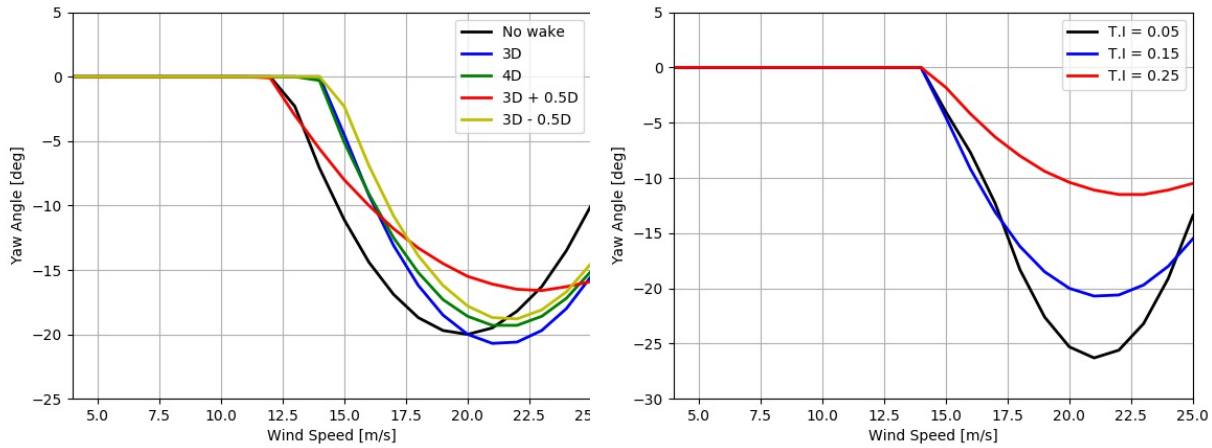

Figure 19: Left: Yaw strategy for same atmospheric conditions (ti = 15%) but different wake upstream positions. Right: Yaw strategy for same upstream wake position (full wake 3D) using different atmospheric turbulence intensities

Low turbulence intensity sites have a larger potential for load alleviation. For example, a 35 % load reduction in the 1 Hz flapwise DEL is observed for high wind speeds at 3D full wake at 5 % turbulence intensity. The higher the turbulence intensity is, the smaller the potential load reduction is. Turbine and site specific reductions are found dependent on the park layout, machine and wind distribution.

The loading on other relevant channels has been assessed presenting small differences compared to the reference (aligned) case. Figure 20 presents the lifetime fatigue equivalent load for the blade flapwise moment (black), blade edgewise moment (blue), tower top for-aft moment (red) and tower top side-side (green). The simulation shows that it is possible to reduce the blade flapwise fatigue loading with minor negative impact on other channels. On the presented results, tower for-aft lifetime DEL was also decreased while blade edgewise and tower side-side were slightly increase (less than 0.1%).

1.5.8 Optimization based on load alleviation

This strategy compromises power in benefit of reducing loading. In figure 12, it is possible to observe the load increment when there is presence of wake. This chapter, presents various examples to illustrate this strategies.

- both derating strategies (pitch, pitch + torque) are comparable. - yaw control is better in forest cases for both blade and shaft loads - proportional derating is generally better in offshore cases for both blade and shaft loads.

Most of the simulations in this project were performed on a 2.3MW machine with a diameter 90 meters. The effects on a larger, more modern, wind turbines has also been evaluated in the project. The DTU 10 MW reference wind turbine, with a rotor diameter of 178m, has been simulated to evaluate the potential load alleviation on bigger turbines.

Figure 23 shows the normalized (using aligned case) blade flapwside DEL for two turbines: DTU 2.3MW

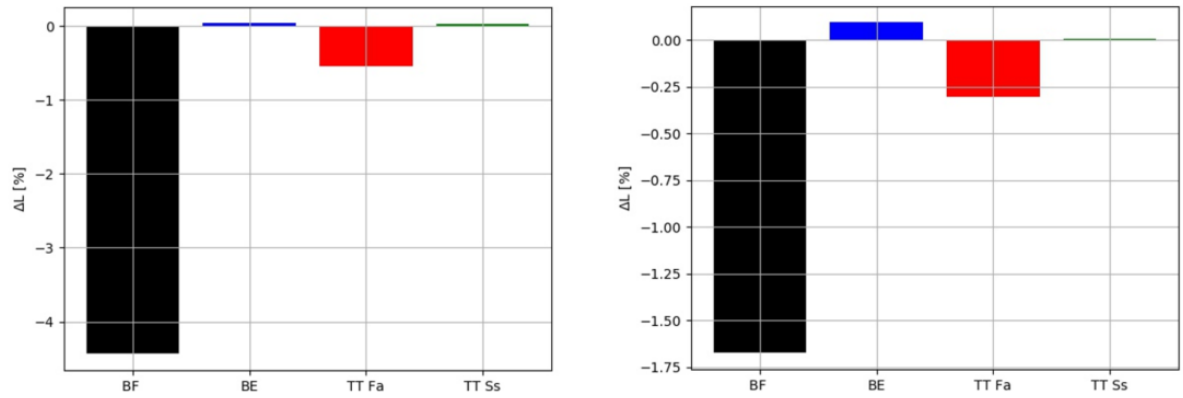

Figure 20: Lifetime DEL using the optimal yaw controller for a non-wake case (left) and a waked case (right) at TI of 15%, Weibull parameter A=8 m/s and k=2

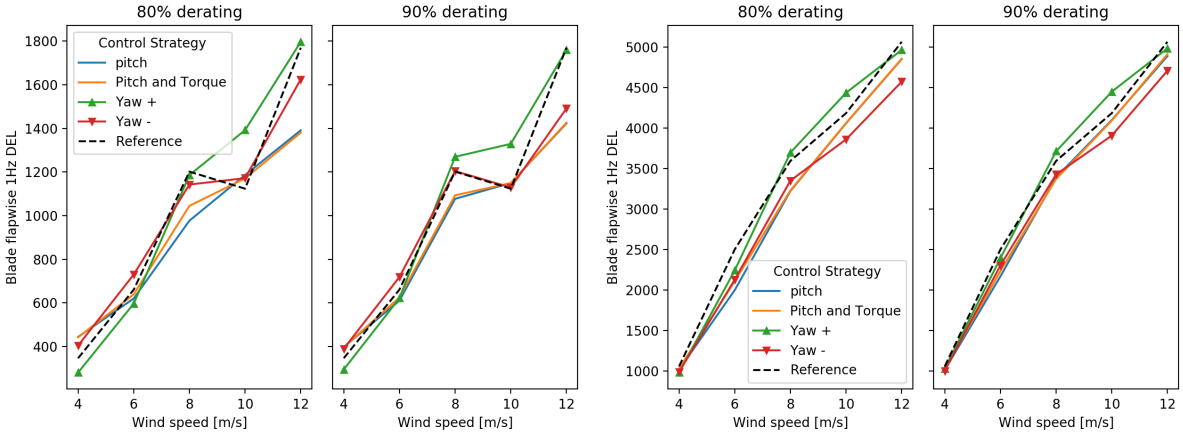

(a) Offshore case

(b) Forest case

Figure 21: Blade flapwise loads

(left) and DTU 10MW (right). It is possible to observe the difference in the load range, towards high wind speed angles, where the biggest turbine presents a higher potential for load alleviation. The geometric properties and aerodynamic design influences the potential of load reduction by intentional misalignment but, as larger is the rotor, larger is the load alleviation.

1.6 Utilization of project results

The outcome of this project is provided in the retrofit market and to co-development projects with turbine manufacturers.

For the retrofit market, the outcome of this project has been implemented at the WindTimizer feature of the 2-beam WindEYE lidar. The WindTIMIZER is Windar Photonics solution for retrofit lidar assisted yaw turbine control.

WindTIMIZER feeds the controller (PLC) with lidar corrected relative wind direction measurements. Figure 24 illustrates WindTIMIZER connection to the turbine controller. The WindTimizer calculates long-term statistics of the correlation between the sensors and the lidar relative wind direction, thus in case of low lidar availability, the yaw misalignment is still corrected with offset added to the sensor measurements.

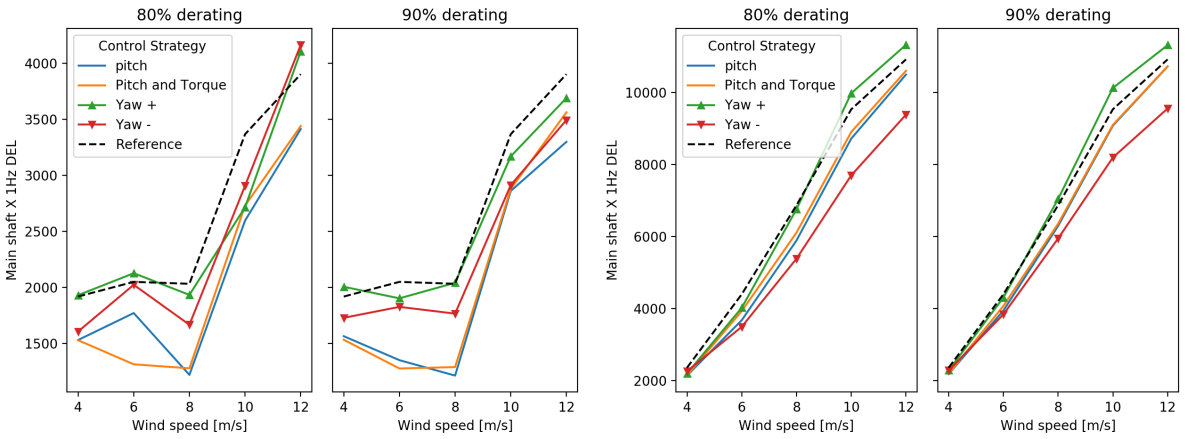

(a) Offshore case

(b) Forest case

Figure 22: Main shaft loads

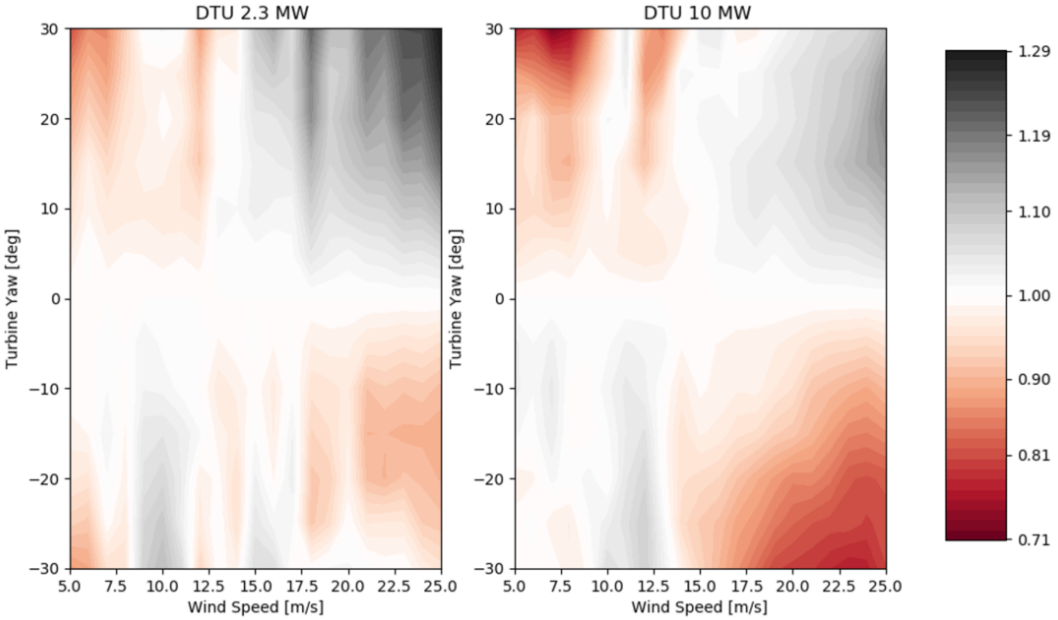

Figure 23: Comparison DTU 2.3 and 10MW normalized DEL blade flapwise loads using atmospheric turbulence intensity 15% and shear 0.2

The lidar misalignment measurements are biased at a wake situation, but the wake detection algorithm can accurately identify these cases. In wake-affected inflow the WindTIMIZER feeds the PLC with corrected yaw measurements from the turbine sensors, similar to what happens at low availability cases. This approach assumes that the turbine sensors relative direction is not affected by wake. We tested this assumption in numerous WindEYE installations around the globe, using SCADA data provided by the turbine owners. It can be verified that the traditional turbine instrumentation, mounted behind the rotor, is not affected by wake inflow in terms of yaw misalignment measurements. Figure 24 illustrates the measured misalignment by the primary sensor, the secondary sensor and WindEYE lidar in a flat terrain site in Canada. The neighboring turbine is located 220^o southwest of the test turbine and affects only lidar misalignment measurements.

A new version of the WindTimizer feature has been developed as an outcome of this project. The wake detection algorithm feeds the WindTimizer with the wake information. When wake is detected, Wind-

Timizer uses the corrected turbine sensor measurements for misalignment information. Based on the wind speed, the wake information and the selected yaw strategy, WindTimizer induces misalignment to the turbine to alleviate loads, by introducing offsets to the turbine sensor measurements.

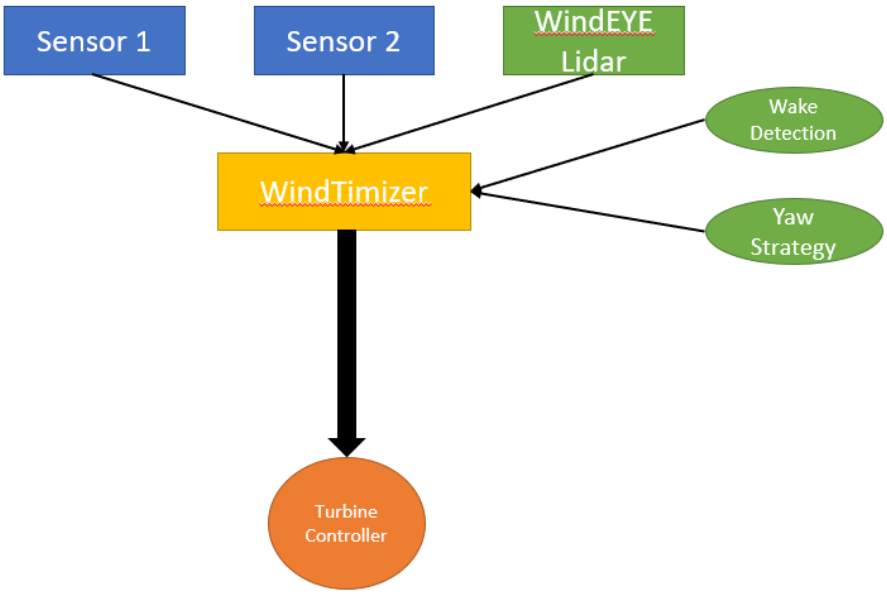

Figure 24: WindTIMIZER connection to the turbine controller

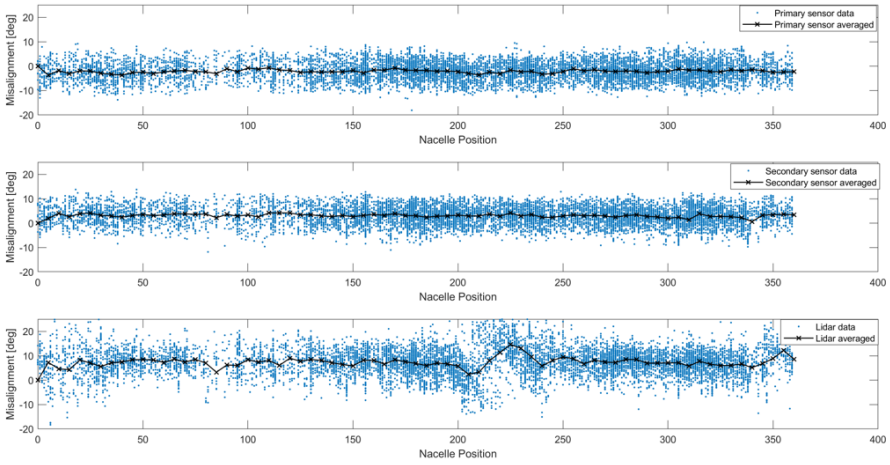

Figure 25: Misalignment as a function of nacelle position for a test turbine in Canada. The wake center is at 220^o

The outcomes of this project, are utilized in direct lidar integration projects with turbine manufacturers, such as the ”Wake Project” with United Power Technology Co.,Ltd. In this project, the lidar feeds the wake detection algorithm output directly to the turbine controller. In the controller level, a module that implements the wake yaw strategy is developed to alleviate loads in wake scenarios.

Summarizing, the work of this project, makes load alleviation in wake scenarios available for turbine manufacturers and the retrofit market, enhancing the optimization capabilities of the nacelle mounted lidars. Moving forward these outcomes can be impemented in a complete wind farm stategy that increases energy yield and decreases turbine loads.

1.7 Project conclusion and perspective

The results we have achieved in the wake project have major impact on our business approach. Throughout our feedback in China Wind Power and Husum Wind, the need for solving wake issues within the wind industry has been highly prioritized, and we have been able to impact some of the decision makers in using LiDAR technology for wake detection.

The recent years there has been a lot of focus within in the wind industry to focus on optimization of individual wind turbines, but more requests are coming up for complete wind farm control and optimization, and here the wake detection project has been important for Windar.

By participating in the wake project Windar has been able to distinguish itself from other LiDAR manufacturers and are now able to offer another essential feature to the LiDAR product.

There shall be no doubt that Windar has been positively surprised about the outcome of the wake project, and to such extend that we have modified our business plan and increased the commercial focus on wake even further.

In a more general level, the technology developed within the frame of this project will also encourage the current energy policy of changing towards renewable sources of energy. Wake detection is an important step for reducing loads on wind turbines. Reduced loads on wind turbines lead to both lower maintenance and the possibility of a slimmer and less expensive turbine design. These factors, in turn, contribute to lowering the cost of wind energy.

We have identified the market need for wake detection and for wake control, and have seen the major market potential the wake scenario has. Almost all wind farms globally have to some extend wake issues, and most of the wind farm / wind turbine manufacturers have so far just accepted the potential power loss by not being able to handle these wake scenarios, but with our ability to measure and potentially to control the wake, we are all of the sudden able to contribute to a new potential increase not only for the wind turbine manufacturers, but also for the IPP (Independent power producers).

The next step for Windar will be to establish a full scale demonstration projects together with a wind turbine manufacturer and an IPP, and document the full scale benefit it will bring to being able to control and adapt to wake situations in the inflow of the turbine.

References

[1] Dominique P Held, Nikolaos Kouris, Antoine Larvol, and Jakob Mann. Wake detection in the turbine inflow using nacelle lidars. *Journal of Physics: Conference Series*, 1102:012005, oct 2018.

[2] D. P. Held and J. Mann. Detection of wakes in the inflow of turbines using nacelle lidars. *Wind Energy Science Discussions*, 2019:1–18, 2019.

[3] Albert M. Urban, Torben J. Larsen, Gunner Chr. Larsen, Dominique P. Held, Ebba Dellwik, and David Robert Verelst. Optimal yaw strategy for optimized power and load in various wake situations: Paper. volume 1102. IOP Publishing, 2018.

[4] Albert M. Urbán, Jaime Liew, Ebba Dellwik, and Gunner Chr. Larsen. The effect of wake position and yaw misalignment on power loss in wind turbines. *Journal of Physics: Conference Series*, 1222:012002, May 2019.

[5] Albert M. Urbán, Torben J. Larsen, Gunner Chr. Larsen, Dominique P. Held, Ebba Dellwik, and David Verelst. Optimal yaw strategy for optimized power and load in various wake situations. *Journal of Physics: Conference Series*, 1102:012019, Oct 2018.

[6] Gunner Chr. Larsen, Helge Madsen Aagaard, Torben J. Larsen, and Niels Troldborg. *Wake modeling and simulation*. Danmarks Tekniske Universitet, Risø Nationallaboratoriet for Bæredygtig Energi, 2008.

[7] Emmanuel Branlard, Anders Tegtmeier Pedersen, Jakob Mann, Nikolas Angelou, Andreas Fischer, Torben Mikkelsen, M. Harris, C. Slinger, and B. F. Montes. Retrieving wind statistics from average spectrum of continuous-wave lidar. *Atmospheric Measurement Techniques*, 6:1673–1683, 2013. Author(s) 2013. This work is distributed under the Creative Commons Attribution 3.0 License.

[8] Knud a. Kragh, Paul a. Fleming, and Andrew K. Scholbrock. Increased Power Capture by Rotor Speed–Dependent Yaw Control of Wind Turbines. *Journal of Solar Energy Engineering*, 135(3):031018, 2013.

[9] Frederik Zahle and Niels N. Sørensen. Characterization of the unsteady flow in the nacelle region of a modern wind turbine. *Wind Energy*, 14(2):271–283, mar 2011.

[10] Gunner Chr Larsen and Kurt S. Hansen. Full-scale measurements of aerodynamic induction in a rotor plane. *Journal of Physics: Conference Series*, 555(1):012063, dec 2014.

[11] T. Mikkelsen, N. Angelou, K. Hansen, M. Sjöholm, M. Harris, C. Slinger, P. Hadley, R. Scullion, G. Ellis, and G. Vives. A spinner-integrated wind lidar for enhanced wind turbine control. *Wind Energy*, 16(4):625–643, may 2013.

[12] Knud a. Kragh, Morten H. Hansen, and Torben Mikkelsen. Improving Yaw Alignment Using Spinner Based LIDAR. *AIAA Aerospace Sciences Meeting including the New Horizons Forum and Aerospace Exposition*, (January):1–13, 2011.

[13] Ervin A. Bossanyi, A Kumar, and O Hugues-Salas. Wind turbine control applications of turbine-mounted LIDAR. *Journal of Physics: Conference Series*, 555:012011, dec 2014.

[14] P. A. Fleming, A. K. Scholbrock, A. Jehu, S. Davoust, E. Osler, A. D. Wright, and A. Clifton. Field-test results using a nacelle-mounted lidar for improving wind turbine power capture by reducing yaw misalignment. *Journal of Physics: Conference Series*, 524(1):012002, jun 2014.

[15] Gunner C Larsen, Helge Aagaard Madsen, F Bingol, Jacob Mann, S. Ott, J. N. Sørensen, V Okulov, Niels Troldborg, Morten Nielsen, Kenneth Thomsen, Torben J. Larsen, and R Mikkelsen. Dynamic wake meandering modeling. Technical Report June, Risø National Laboratory Technical University of Denmark, Risø-R-1607(EN), 2007.

[16] Gunner C. Larsen, Helge Aa Madsen, Kenneth Thomsen, and Torben J. Larsen. Wake meandering: A pragmatic approach. *Wind Energy*, 11(4):377–395, 2008.

[17] Ewan Machefaux, Niels Troldborg, Gunner C. Larsen, Jakob Mann, and Helge Aa Madsen. Experimental and numerical study of wake to wake interaction in wind farms. *European Wind Energy Conference and Exhibition 2012, EWEC 2012*, (September):223–232, 2012.

[18] R. E. Kalman. A New Approach to Linear Filtering and Prediction Problems. *Journal of Basic Engineering*, 82(1):35, 1960.

[19] Romeo Ortega, Fernando Mancilla-David, and Fernando Jaramillo. A globally convergent wind speed estimator for wind turbine systems. *International Journal of Adaptive Control and Signal Processing*, 27(5):413–425, may 2013.

[20] Knud Abildgaard Kragh and Morten Hartvig Hansen. Load alleviation of wind turbines by yaw misalignment. *Wind Energy*, 17(7):971–982, 2014.

Wake detection

Presentations on the subject was given at the Global Wind Summit, WindEurope, 2018: https://windeurope.org/summit2018/conference/sessions/?session_id=40.0

- Dominique P Held, Nikolaos Kouris, Antoine Larvol, and Jakob Mann. Wake detection in the turbine inflow using nacelle lidars. *Journal of Physics: Conference Series*, 1102:012005, oct 2018
- D. P. Held and J. Mann. Detection of wakes in the inflow of turbines using nacelle lidars. *Wind Energy Science Discussions*, 2019:1–18, 2019

Optimization of wind turbine control in wake situations

Presentations on the subject was given at the Global Wind Summit, WindEurope, 2018: https://windeurope.org/summit2018/conference/sessions/?session_id=40.0 and at the WindEurope conference and exhibition in Bilbao, April 2nd - 4th, 2019.

- Albert M. Urbán, Torben J. Larsen, Gunner Chr. Larsen, Dominique P. Held, Ebba Dellwik, and David Verelst. Optimal yaw strategy for optimized power and load in various wake situations. *Journal of Physics: Conference Series*, 1102:012019, Oct 2018
- Albert M. Urbán, Jaime Liew, Ebba Dellwik, and Gunner Chr. Larsen. The effect of wake position and yaw misalignment on power loss in wind turbines. *Journal of Physics: Conference Series*, 1222:012002, May 2019

Other dissemination and marketing

- Vestas Wind, Dec 2017
- Envision Energy, Nov 2017
- DongFang, May 2018
- HEAG, April 2018
- CSIC, June 2018
- China Wind Power, Beijing, October 2018
- United Power, Nov 2018
- WindEurope, Barcelona, April 2019

B: Generic structure of wake deficits and wake generated turbulence profiles